communications physics

Article

https://doi.org/10.1038/s42005-024-01555-3

Verification of ultrafast spin transfer effects in iron-nickel alloys

Christina Möller[1], Henrike Probst[1], G. S. Matthijs Jansen[1] ✉, Maren Schumacher[1], Mariana Brede[1], John Kay Dewhurst[2], Marcel Reutzel[1], Daniel Steil[1], Sangeeta Sharma[3] & Stefan Mathias[1] ✉

The optical intersite spin transfer (OISTR) effect was recently verified in $Fe_{50}Ni_{50}$ using extreme ultraviolet magneto-optical Kerr measurements. However, one of the main experimental signatures analyzed in this work, namely a magnetic moment increase at a specific energy in Ni, was subsequently found also in pure Ni, where no transfer from one element to another is possible. Hence, it is a much-discussed issue whether OISTR in FeNi alloys is real and whether it can be verified experimentally or not. Here, we present a comparative study of spin transfer in $Fe_{50}Ni_{50}$, $Fe_{19}Ni_{81}$ and pure Ni. We conclusively show that an increase in the magneto-optical signal is indeed insufficient to verify OISTR. However, we also show how an extended data analysis overcomes this problem and allows to unambiguously identify spin transfer effects. Concomitantly, our work solves the long-standing riddle about the origin of delayed demagnetization behavior of Ni in FeNi alloys.

The ability to drive spin dynamics by ultrashort laser pulses offers a unique opportunity to bring the field of spintronics into the femtosecond regime, as demonstrated, for example, by the successful application of superdiffusive spin currents[1–4] in spintronic emitters[5] and the possibility of direct magnetic phase switching by femtosecond laser pulses[6–8]. Recently, a fascinating discovery was made in this context: given a suitable material, it is possible to drive spin transfer between sublattices directly by a strong optical field[9–14]. This process, called optical intersite spin transfer (OISTR), even precedes the ultrafast demagnetization process and thus provides a path to even faster spintronic applications[15].

OISTR was first proposed theoretically by the Sharma group[16] and has meanwhile been experimentally verified in a number of experiments. In the OISTR process, an ultrafast optical excitation drives spin-preserving electronic transitions from below the Fermi level to above the Fermi level. Due to the exchange-split bands in ferromagnets, different numbers of spin-up and spin-down electrons are excited by the laser pulse, which leads to an ultrafast spectral redistribution of the electron density as well as to an ultrafast spectral redistribution of the spins and thus to ultrafast dynamics in the spin-polarization. If the initial states for such an excitation are predominantly found in one elementary subsystem, e.g., of an alloy, and the final states are predominantly found in another elementary subsystem, an intersite spin transfer occurs, which offers the potential for advanced and extremely fast control of magnetic behavior.

One of the first experiments to verify the OISTR effect was an experiment on an $Fe_{50}Ni_{50}$ alloy using the ultrafast transverse magneto-optical effect (T-MOKE) in the extreme ultraviolet (EUV) region[9]. The T-MOKE experiment showed a spectrally dependent increase in magnetic asymmetry in Ni and a concomitant decrease in Fe, and the corresponding transient dynamics of majority and minority spin occupation in the $Fe_{50}Ni_{50}$ alloy were calculated by time-dependent density functional theory (TDDFT). However, doubt was recently cast on this experimental signature, as a similar ultrafast increase in Ni has recently also been observed in pure Ni material[17,18], where spin transfer to another subsystem is not possible. On the one hand, such a signature is not unexpected, since ultrafast excitation also drives occupation changes in pure materials[19], but on the other hand, the question arises to what extent the observed increase in the magnetic asymmetry is a valid signature to verify spin transfer from Ni to the Fe in $Fe_{50}Ni_{50}$. The situation is further complicated by the fact that identical magnetization dynamics can appear drastically different in EUV T-MOKE depending on the precise experimental geometry[18]. The critical question is therefore whether OISTR can experimentally be verified in $Fe_{50}Ni_{50}$.

In this work, we present new data and a new quantitative analysis on this topic in a comparative experimental and theoretical study of laser-driven spin transfer processes in $Fe_{50}Ni_{50}$, $Fe_{19}Ni_{81}$ (permalloy), and pure Ni (see Fig. 1). We revisit the previously observed signatures of the OISTR effect and, following the approach that we developed in ref. 18, perform a full time-resolved reconstruction of the dielectric tensor. This allows us to directly

[1]I. Physikalisches Institut, Georg-August-Universität Göttingen, Friedrich-Hund-Platz 1, 37077 Göttingen, Germany. [2]Max Planck Institute of Microstructure Physics, Weinberg 2, 06120 Halle, Germany. [3]Max-Born-Institute for Non-linear Optics and Short Pulse Spectroscopy, Max-Born Strasse 2A, 12489 Berlin, Germany. ✉e-mail: gsmjansen@uni-goettingen.de; smathias@uni-goettingen.de

compare the same quantity obtained from experiment and theory: namely, the transient dynamics in the dielectric tensor. We find that in all three materials signatures of the ultrafast laser-driven spectral redistribution of spins can be clearly identified. Furthermore, we find that the amplitude of these dynamics at the Ni site increases with increasing Fe content in the alloy, supporting the OISTR description. In the case of $Fe_{50}Ni_{50}$, we experimentally verify the transfer of minority spins from the Ni subsystem to the Fe subsystem, i.e., the OISTR effect. Finally, we are also able to explain the origin of the much-discussed delayed demagnetization behavior of Fe and Ni in these alloys[20–27].

Results and discussion

We begin with a measurement of $Fe_{19}Ni_{81}$ that very clearly illustrates that an increase in T-MOKE asymmetry in a specific spectral region may not be sufficient to verify spin transfer effects without further analysis. Figure 2a shows energy-resolved magnetic asymmetries measured with EUV T-MOKE of the $Fe_{19}Ni_{81}$ sample for two different incidence angles (θ) of the EUV light. While the asymmetries look quite similar, the zero crossings are slightly shifted so that there are spectral regions where the asymmetry is negative for one angle of incidence and positive for the other, most notably at 52 and 64 eV. Most curiously, we find apparently contradictory ultrafast dynamics of the T-MOKE asymmetry in the time-resolved experiment for these spectral regions: Fig. 2b shows the time-resolved change of the asymmetry as a function of EUV energy at $\theta = 43.4°$. Here, the signal at 63.9 eV (dark blue) shows a time-resolved increase in the T-MOKE asymmetry, which is exactly the signature used to verify the OISTR effect in our previous work. However, in Fig. 2c, for a slightly different angle of incidence ($\theta = 45.1°$), the same spectral region shows the exact opposite behavior, namely an ultrafast decrease. Note that we observe this behavior for all three samples Ni, $Fe_{19}Ni_{81}$, and $Fe_{50}Ni_{50}$ (cf. Supplementary Fig. 1). Clearly, no conclusion should be drawn from these data without further knowledge of the OISTR effect and its signatures in the T-MOKE signal.

To overcome this problem, we apply an extended analysis, based on the experimental determination of the transient dynamics of the dielectric tensor that we developed in ref. 18. This analysis shows that the peculiar behavior of the asymmetry increases and decreases for two different incidence angles is due to a transient rotation of the off-diagonal element of the dielectric tensor (ϵ_{xy}) in the complex plane. If this rotation of ϵ_{xy} happens at photon energies near the zero crossings of the T-MOKE asymmetry, it can lead to opposite dynamics in the magnetic asymmetry due to the projection of ϵ_{xy} onto an angle-dependent probe vector (see ref. 18 for the description of the analysis and the influence of the rotation of ϵ_{xy} on the T-MOKE asymmetry spectra; see Supplementary Fig. 1 for the additional data needed to perform this analysis). Instead, extracting ϵ_{xy} from the angle-dependent T-MOKE asymmetry data has several advantages: (i) the real part of ϵ_{xy} is related to the spin-polarization of the unoccupied states and can also be measured by other techniques, such as X-ray magnetic circular dichroism (XMCD); (ii) the quantity ϵ_{xy} is now independent of the measurement technique or geometry used; (iii) the transient changes in ϵ_{xy} allow a direct comparison with TDDFT calculations.

Figure 3a shows TDDFT calculations[28,29] of the transient dynamics of the spin-resolved occupation in Fe and Ni in the $Fe_{50}Ni_{50}$ sample. A calculation of $Fe_{19}Ni_{81}$ is computationally very costly due to the large required supercell size and was therefore not performed for the present study. The calculations for $Fe_{50}Ni_{50}$ are similar to the results presented in ref. 9, but adapted for the pump pulse energy (1.2 eV) and pulse duration (47 fs) of the present experiment[30]. While the Fe and Ni electrons share a common (metallic) band structure in the alloy, the character of the different states can be projected onto bands originating dominantly from the Ni or Fe subsystem. The OISTR effect then manifests itself in occupation transfer from minority states below the Fermi level with predominantly Ni character to minority states above the Fermi level with predominantly Fe character. Of course, other transitions within the subsystems also contribute to the optical response, but they do not transfer spin from one subsystem to the other subsystem and are therefore not discussed further here. Transitions between the subsystems within the majority channel are also possible, but these are only minor changes compared to the strong changes in the minority channel (cf. Supplementary Fig. 3). As can be seen from these calculations, there is a spectral region below the Fermi level that shows a depletion of minority spins for states with a predominant Ni character, leading to an increase in

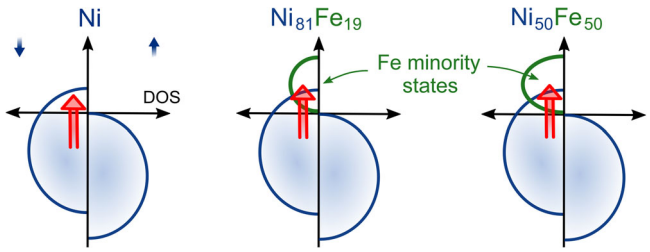

Fig. 1 | Simplified illustration of the 3d states in Ni, $Fe_{19}Ni_{81}$, and $Fe_{50}Ni_{50}$. The addition of Fe in the alloys leads to additional unoccupied states in the minority channel that can be populated through optical intersite spin transfer (OISTR). Time-dependent density functional theory calculations predict a stronger OISTR effect in $Fe_{50}Ni_{50}$ compared to $Fe_{19}Ni_{81}$ due to the larger amount of available Fe states above the Fermi level[35]. On the other hand, in elemental Ni, the OISTR process is not possible.

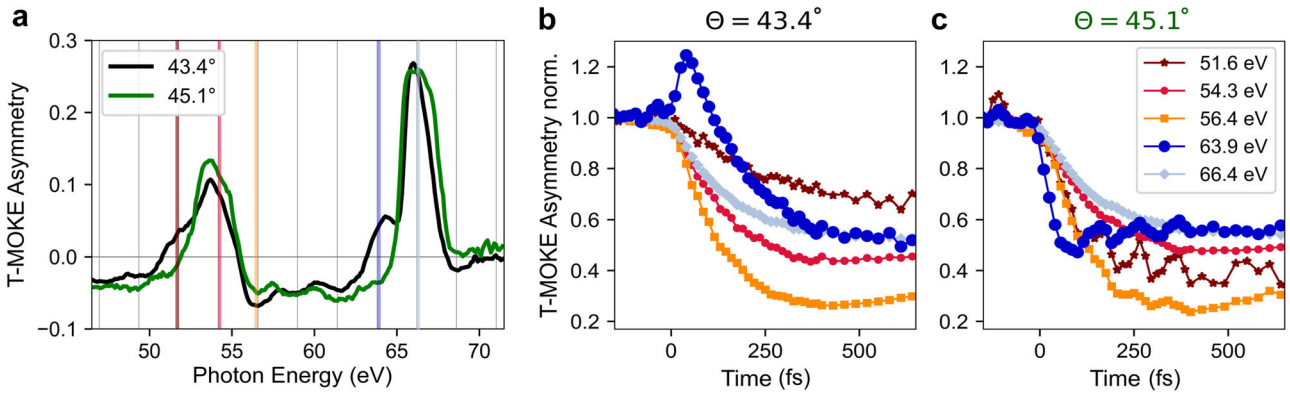

Fig. 2 | Apparently contradictory extreme ultraviolet transverse magneto-optical Kerr effect (EUV T-MOKE) measurements of optical intersite spin transfer (OISTR) in $Fe_{19}Ni_{81}$, recorded at different EUV incidence angles and otherwise identical conditions (the data of $Fe_{50}Ni_{50}$ and Ni can be found in the Supplementary Fig. 1). a Static T-MOKE asymmetry for two incidence angles. Note that the magnetic asymmetry changes sign around 52 eV and 64 eV for the two different incidence angles. **b**, **c** Time-resolved magnetic asymmetry traces for 43.4° and 45.1° incidence angle, respectively. The analyzed photon energies around the M absorption edges of Fe (54.2 eV) and Ni (66 eV) are marked as colored bars in (**a**). At 43.4°, the typical transient increase at 63.9 eV that was previously associated with OISTR is seen[9], while no such increase is visible at 45.1°.

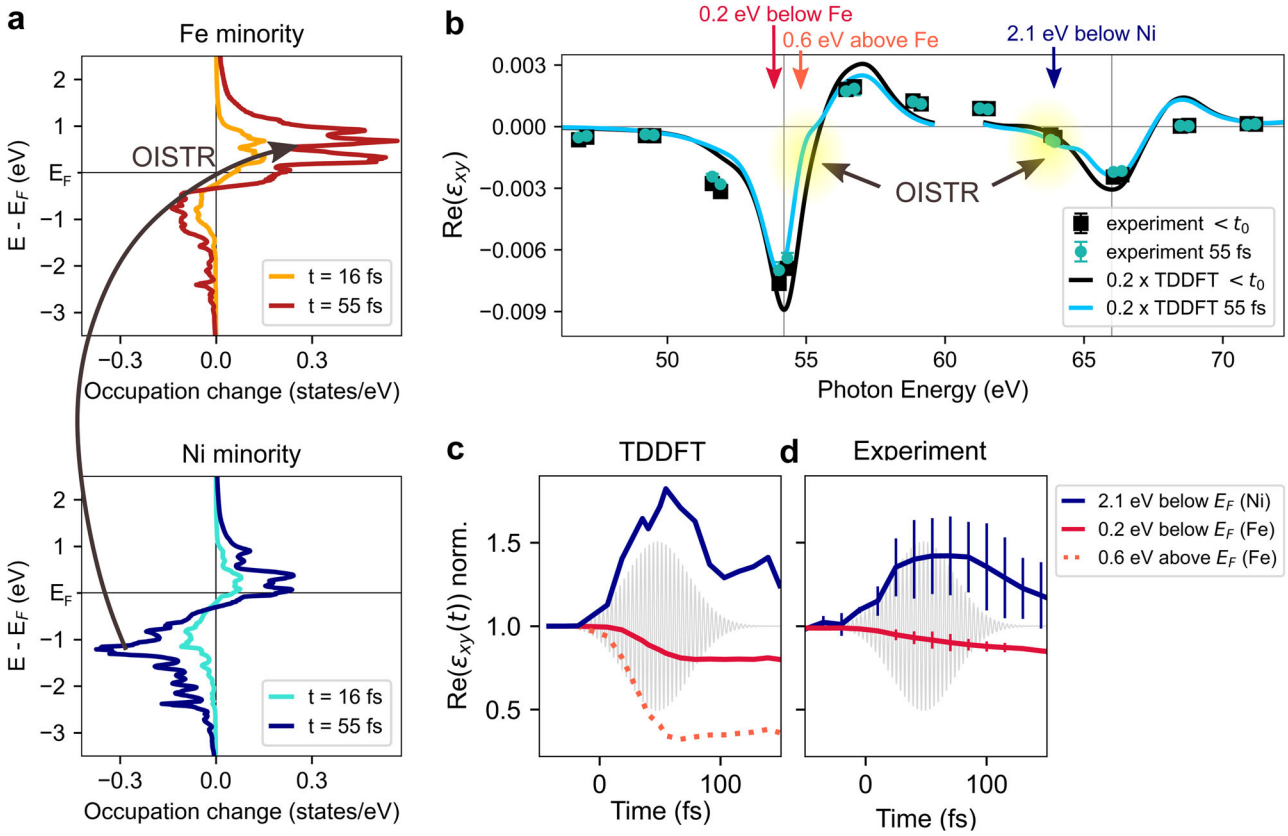

Fig. 3 | Time-dependent density functional theory (TDDFT) calculations of OISTR in $Fe_{50}Ni_{50}$, compared to experiment. a The transient occupation change of minority spins at the Ni and Fe sites in $Fe_{50}Ni_{50}$. The OISTR process excites minority spins in Ni from below the Fermi edge E_F to Fe minority states above the Fermi edge. **b** Comparison of the static ($< t_0$) off-diagonal dielectric tensor element to the transient state at 55 fs, as extracted from the measured magneto-optical spectroscopy data (points) and TDDFT calculations (lines). For the red, orange, and blue arrows, 54.2 eV and 66 eV were used for the M edges of Fe and Ni, respectively, which allows to reference the energy scale to the Fermi level. **c**, **d** The transient evolution of the real part of ϵ_{xy} is shown at specific energies referenced to the Fermi level from TDDFT and experiment, respectively. For quantitative comparison, ϵ_{xy}(t) was normalized to its value before the pump pulse arrives. The error margins in (**d**) indicate the statistical error margins as retrieved from the fitting procedure. The statistical errors in (**b**) are smaller than the symbol size and therefore not visible.

the energy-resolved magnetic moment at the Ni site. Conversely, there are spectral regions above the Fermi level of the Fe states where the increase in minority spins leads to a rapid quenching of the energy-resolved magnetic moment. Hofherr et al.[9] found two similar features in the time-resolved asymmetry and interpreted them as indicators of the OISTR effect.

However, for the reasons given above, we now go one step further and calculate from TDDFT the signature of OISTR on the transient dynamics of the dielectric tensor[31,32]. Figure 3b shows the real part of ϵ_{xy} from theory (lines) and experiment (points) for two exemplary pump-probe delays (before time zero and at 55 fs). The first important observation from the calculated time- and spectrally resolved Re(ϵ_{xy}) data is that the spectrally very distinct dynamics in the spin-resolved DOS (Fig. 3a) are strongly broadened. This is due to the intrinsic linewidth of the 3p core levels and their partial overlap. Nevertheless, the second important observation is that it is still possible to pinpoint the OISTR effect from the theory data: For photon energies between 63.0 eV and 64.4 eV, there is a relative increase in Re(ϵ_{xy}) caused by the pump-induced ultrafast loss of minority spins in Ni. Conversely, in the 55 eV energy region, Fe shows a rapid decrease in Re(ϵ_{xy}) on the timescale of the pump pulse due to the addition of transferred minority spins originating from Ni states.

Figure 3c summarizes the expected transient behavior of Re(ϵ_{xy}) from TDDFT for the discussed energies, with the blue curve showing the increase in Ni and the orange dotted curve showing the corresponding rapid decrease in Fe, now approximately referenced to the Fermi levels of Ni and Fe, respectively, by subtracting the respective M-edge energies from the photon energies (cf. Fig. 3b for the corresponding photon energies). In direct comparison, Fig. 3d shows the experimentally extracted transient dynamics of Re(ϵ_{xy}) for respective photon energies. First, we see that we are able to verify the important increase in Re(ϵ_{xy}) in experiment, which is indicative of the loss of minority spins in Ni due to optical pumping (blue line). Second, however, we do not have sufficient EUV intensity in the important spectral region just above the Fe M-edge, which is expected to show the strong and rapid decrease due to the increase of minority spins above the Fermi level (orange dotted line in theory, Fig. 3c, absent in experiment, Fig. 3d). The next available EUV harmonic with sufficient intensity in our experimental data is at 0.2 eV below Fe M-edge, and we find good qualitative agreement with theory (red lines in Fig. 3c, d). However, there is also a qualitative discrepancy with respect to timescales larger than 80 fs, where the theoretical magnetization remains constant while the experimental magnetization decreases. This can be understood by considering the limitations of the TDDFT calculations: TDDFT is well suited to describe the very early magnetization dynamics induced by the pump pulse and in particular the excitation. On longer timescales, however, the well-known demagnetization processes evolve, not all of which are included in TDDFT. In particular, Elliott-Yafet spin-flip electron–phonon scattering[33] is not included in TDDFT, which explains that TDDFT does not capture the full magnetization decrease for timescales >80 fs. In summary, we can clearly verify the loss of minority spins in the Ni subsystem from these experimental data, but we have no experimental evidence that these spins are transferred to the Fe subsystem.

For the present work, we therefore take another approach and aim to compare the spectrally resolved T-MOKE data of pure Ni (These data are reproduced from refs. [18,34], where we describe the ϵ_{xy} analysis procedure in detail), where only an inter-energy spin transfer is involved, with data from

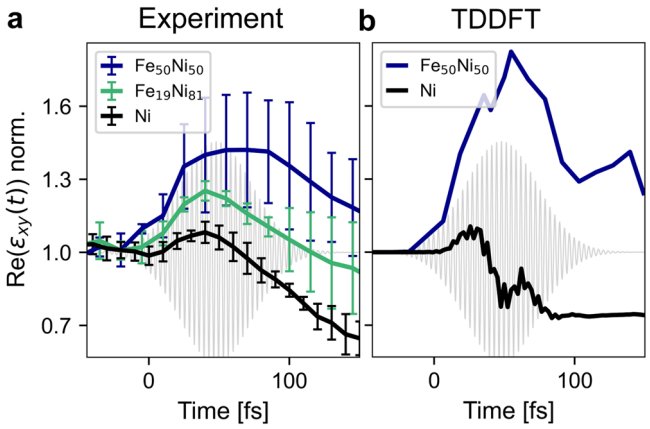

Fig. 4 | Comparison of the transient off-diagonal tensor element Re(ϵ_{xy}) for 63.9 eV for $Fe_{50}Ni_{50}$, $Fe_{19}Ni_{81}$ and Ni. a As extracted from the measured magneto-optical spectroscopy data. **b** As calculated by time-dependent density functional theory. The error margins in (**a**) indicate the statistical error margins as retrieved from the fitting procedure. The spin transfer between Ni and Fe is visible by an increase of Re(ϵ_{xy}) at 63.9 eV, which probes Ni minority states below the Fermi level. In experiment, the spin transfer is found to be more efficient in $Fe_{50}Ni_{50}$ than in $Fe_{19}Ni_{81}$. In Ni, minority electrons are excited from below to above the Fermi level, which results in a short and comparatively small increase of Re(ϵ_{xy}).

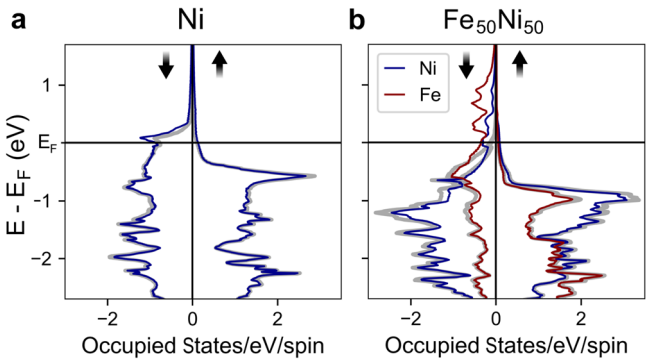

Fig. 5 | Occupied minority and majority states before and after the optical excitation, calculated with time-dependent density functional theory. a Spin-resolved occupation in Ni before optical excitation in gray, and $t = 55$ fs after optical excitation in blue. **b** Corresponding plot for $Fe_{50}Ni_{50}$, where the $t = 55$ fs occupation at the Fe sites is shown in red.

$Fe_{19}Ni_{81}$ and $Fe_{50}Ni_{50}$, where an intersite spin transfer between Ni and Fe becomes possible and is predicted by theory (for the $Fe_{50}Ni_{50}$ alloy). Figure 4a shows the experimentally analyzed transient change of Re(ϵ_{xy}) for the spectral region where the OISTR-induced increase was expected and verified in the case of $Fe_{50}Ni_{50}$ (blue). Compared to $Fe_{50}Ni_{50}$, the increase in $Fe_{19}Ni_{81}$ (green) is much less pronounced and in pure Ni, it is mostly seen as a delay (black). From these data, we can directly conclude that the OISTR-relevant transition is most efficiently excited in the $Fe_{50}Ni_{50}$, less efficiently in $Fe_{19}Ni_{81}$, and even less in Ni. In comparison with theory (Fig. 4b), we again find good qualitative agreement for $Fe_{50}Ni_{50}$ as discussed above, but also for Ni (see Supplementary Figs. 4–6 for further comparison of EUV T-MOKE and TDDFT). Note that the absorbed fluence and the quenching of the transient asymmetry are not the same for all three measurements (cf. "Methods" and Supplementary Fig. 1).

To shed light on the origin of the observed differences in excitation efficiencies in the minority channels, we take a closer look at the band structure of these materials, and possible excitation pathways. Figure 5a shows the spin-resolved density of states for pure Ni material. In Ni, more (spin-conserving optical) excitations are possible in the minority channel than in the majority channel. These transitions are captured in theory and experiment by a loss of minority spins below the Fermi level, and lead to the observed small increase for Re(ϵ_{xy}) at ≈ 2.1 eV below the Ni edge. In the case of $Fe_{50}Ni_{50}$, as shown in Fig. 5b, the situation is different. Here, the addition of Fe adds additional final states above the Fermi level in the minority channel. Thus, a first glance at the band structure suggests that additional transitions from the Ni minority states below the Fermi level to the Fe minority states above the Fermi level become possible. According to theory, this is indeed the case and leads to the strong relative increase of Re(ϵ_{xy}) at 2.1 eV below the Ni edge and, in addition, to a rapid relative decrease of Re(ϵ_{xy}) just above the Fe edge. While we cannot probe the rapid decrease with the given EUV light source in our experiment, we very well reproduce the modified efficiency of the OISTR transition and therefore conclude that the experiment also shows that in $Fe_{50}Ni_{50}$ OISTR is operative, i.e., minority spins from Ni are indeed pumped into minority states of Fe by the ultrafast laser excitation.

Next, we see that the $Fe_{19}Ni_{81}$ alloy, according to the experiment (see Fig. 4a), lies between the situation of Ni, where no intersite spin transfer is possible, and $Fe_{50}Ni_{50}$, where OISTR is apparently strong. Using the same reasoning as above, one would expect some amount of Fe DOS above the Fermi level but less than in the case of $Fe_{50}Ni_{50}$. Indeed, such a series of spin-resolved DOS has already been calculated in ref. 35 and is in full agreement with the expectations and observations developed above.

Finally, we would like to note that the addition of Fe in Fe–Ni alloys not only increases the number of Fe minority final states above the Fermi level but also modifies the Ni-projected DOS and occupation (Fig. 5). Therefore, not only the OISTR transition becomes possible and is amplified with increasing Fe content, but also transitions localized to the Ni subsystem are modified, which might also contribute to the observed changes in the transient Re(ϵ_{xy}) in Fig. 4. However, we derive from the TDDFT calculations that the loss of minority spins due to Ni–Ni minority transitions is nearly identical in Ni and $Fe_{50}Ni_{50}$, and can therefore not explain the observed stronger increase in our $Fe_{50}Ni_{50}$ data (see Supplementary Discussion 1 and Figures therein). In other words, the stronger increase for $Fe_{50}Ni_{50}$ in Fig. 4 is unambiguously caused by the additional Ni minority to Fe minority transitions, i.e., the OISTR effect, and the difference to the weaker increase of Re(ϵ_{xy}) in Ni is a direct indication of its strength in $Fe_{50}Ni_{50}$ and $Fe_{19}Ni_{81}$.

We also would like to discuss our new results in relation to the results on permalloy obtained in the last decade with EUV T-MOKE (Mathias et al.[20], Günther et al.[21] and the supplemental material therein, Jana et al.[25]). In these works, Fe and Ni showed a delayed demagnetization behavior with identical demagnetization time constants, which was recently verified in XMCD experiments at the L-edges of Fe and Ni[27]. The identical demagnetization time constants for Fe and Ni aren't surprising: Fe and Ni are strongly exchange-coupled in these alloys. However, the important question has always been what causes the delay between the two subsystems. The interpretation of the OISTR process induced by the pump pulse now makes this clear. OISTR initiates a non-equilibrium between the Ni and Fe subsystems via the transfer of minority spins on the very short timescale of the pump excitation. Subsequently, demagnetization occurs via the well-known spin-flip and exchange scattering processes, and both subsystems start to demagnetize at the same rate. At the time of the first experiment[20], the small increase due to OISTR in permalloy was not resolved, but the subsequent delayed behavior in the demagnetization of the Fe and Ni subsystems was clearly identified. However, for the reasons given above, we also revisit the delayed demagnetization of Ni and Fe and perform an energy-integrated analysis of Re(ϵ_{xy}). From this extended analysis, we still find a demagnetization delay for Ni in $Fe_{19}Ni_{81}$ of 12 ± 3 fs, while $Fe_{50}Ni_{50}$ actually shows both a transient increase in Ni and a relative delay of 95 ± 7 fs (see Supplementary Discussion 2 for the transient dynamics of Re(ϵ_{xy})). Here, we note that the increased delayed behavior is not a consequence of a statically modified exchange coupling, as was previously found for permalloy alloyed with Cu[20]. In $Fe_{50}Ni_{50}$ and $Fe_{19}Ni_{81}$, the exchange

coupling is the same, but the OISTR is strongly modified and this leads to a stronger delayed behavior in $Fe_{50}Ni_{50}$.

In conclusion, we have carried out a combined experimental-theoretical analysis of optically-driven spin transfer in Ni, $Fe_{19}Ni_{81}$, and $Fe_{50}Ni_{50}$. We have paid special attention to the observed increase and delay of the magnetic asymmetry in T-MOKE, which was found in the alloys, but also in pure Ni material. Through an extended analysis (see ref. 18), we are able to directly compare transient dynamics in the real part of the off-diagonal element of the dielectric tensor $\mathrm{Re}(\epsilon_{xy})$. Crucially, this procedure allows us to make a direct comparison with TDDFT theory calculations, which helps us to identify and explain all the observed signals. In summary, we verify OISTR in $Fe_{50}Ni_{50}$ and elucidate the origin of the previously found delays in these material systems.

Methods

Sample characteristics

In this study, we have measured magnetization dynamics in three different samples: $Fe_{50}Ni_{50}$, $Fe_{19}Ni_{81}$ and pure Ni. For the determination of ϵ_{xy} from angle-resolved T-MOKE data, the sample composition must be known accurately. From X-ray reflectivity and the sample preparation procedures, we find the following sample structures: Si_3N_4(3 nm)/$Fe_{50}Ni_{50}$(15 nm)/SiO_2(100 nm)/Si, Si_3N_4(5 nm)/$Fe_{19}Ni_{81}$(15 nm)/SiO_2(100 nm)/Si, NiO(2 nm)/Ni(22 nm)/Si_3N_4(112 nm)/SiO_2. The Fe–Ni samples were grown by magnetron sputtering. The Ni sample was obtained by Ar ion beam sputtering using a Kaufman source. In order to saturate the magnetization in the EUV T-MOKE measurement, we used an in-plane external magnetic field with a strength of ± 0.1 T.

EUV T-MOKE data for Fe–Ni alloys and Ni

We measured the transient T-MOKE asymmetry for multiple incidence angles in order to be able to extract the transient off-diagonal tensor element $\mathrm{Re}(\epsilon_{xy})$. The reflected 100 kHz EUV probe beam spans energies between 30 and 72 eV (see Supplementary Fig. 2 for a complete spectrum). We estimate the resolution of the spectrometer to be better than 0.2 eV, while the photon energy calibration is accurate to <2%. Details on the angle-resolved measurement and analysis are given in ref. 18, while general information on the experimental setup can be found in ref. 26.

The experimental T-MOKE asymmetries and their dynamics for $Fe_{50}Ni_{50}$, $Fe_{19}Ni_{81}$, and Ni are shown in Supplementary Fig. 1. Here, we pumped the samples with a 47 ± 5 fs pulses (Gauss FWHM) with a photon energy of 1.2 eV. The absorbed fluence is slightly different for each measurement: $0.8 \pm 0.2^{\mathrm{mJ}/\mathrm{cm}^2}$ for Ni, $1.1 \pm 0.2^{\mathrm{mJ}/\mathrm{cm}^2}$ for $Fe_{50}Ni_{50}$ and $0.8 \pm 0.2^{\mathrm{mJ}/\mathrm{cm}^2}$ for $Fe_{19}Ni_{81}$.

Data availability

The data and analysis scripts that support the findings of this study are available on the GRO.Data platform. The static and time-resolved ϵ_{xy} analysis for the $Fe_{19}Ni_{81}$ and $Fe_{50}Ni_{50}$ samples, as well as the comparison of the experimental data with the TDDFT results can be found in ref. 36. The static and time-resolved ϵ_{xy} analysis of the Ni sample can be found in ref. 34.

Received: 16 June 2023; Accepted: 8 February 2024;
Published online: 02 March 2024

References

1. Malinowski, G. et al. Control of speed and efficiency of ultrafast demagnetization by direct transfer of spin angular momentum. *Nat. Phys.* **4**, 855–858 (2008).
2. Rudolf, D. et al. Ultrafast magnetization enhancement in metallic multilayers driven by superdiffusive spin current. *Nat. Commun.* **3**, 1037 (2012).
3. Battiato, M., Carva, K. & Oppeneer, P. M. Superdiffusive spin transport as a mechanism of ultrafast demagnetization. *Phys. Rev. Lett.* **105**, 027203 (2010).
4. Melnikov, A. et al. Ultrafast transport of laser-excited spin-polarized carriers in Au/Fe/MgO (001). *Phys. Rev. Lett.* **107**, 076601 (2011).
5. Seifert, T. et al. Efficient metallic spintronic emitters of ultrabroadband terahertz radiation. *Nat. Photon* **10**, 483–488 (2016).
6. Stanciu, C. D. et al. All-optical magnetic recording with circularly polarized light. *Phys. Rev. Lett.* **99**, 047601 (2007).
7. Lambert, C.-H. et al. All-optical control of ferromagnetic thin films and nanostructures. *Science* **345**, 1337–1340 (2014).
8. Schlauderer, S. et al. Temporal and spectral fingerprints of ultrafast all-coherent spin switching. *Nature* **569**, 383–387 (2019).
9. Hofherr, M. et al. Ultrafast optically induced spin transfer in ferromagnetic alloys. *Sci. Adv.* **6**, eaay8717 (2020).
10. Tengdin, P. et al. Direct light-induced spin transfer between different elements in a spintronic Heusler material via femtosecond laser excitation. *Sci. Adv.* **6**, eaaz1100 (2020).
11. Willems, F. et al. Optical inter-site spin transfer probed by energy and spin-resolved transient absorption spectroscopy. *Nat. Commun.* **11**, 871 (2020).
12. Siegrist, F. et al. Light-wave dynamic control of magnetism. *Nature* **571**, 240–244 (2019).
13. Steil, D. et al. Efficiency of ultrafast optically induced spin transfer in Heusler compounds. *Phys. Rev. Res.* **2**, 023199 (2020).
14. Ryan, S. A. et al. Optically controlling the competition between spin flips and intersite spin transfer in a Heusler half-metal on sub–100-fs time scales. Sci. Adv. **9**, eadi1428 (2023).
15. El-Ghazaly, A., Gorchon, J., Wilson, R. B., Pattabi, A. & Bokor, J. Progress towards ultrafast spintronics applications. *J. Magn. Magn. Mater.* **502**, 166478 (2020).
16. Dewhurst, J. K., Elliott, P., Shallcross, S., Gross, E. K. U. & Sharma, S. Laser-induced intersite spin transfer. *Nano Lett.* **18**, 1842–1848 (2018).
17. Hennes, M. et al. Time-resolved XUV absorption spectroscopy and magnetic circular dichroism at the Ni $M_{2,3}$-edges. *Appl. Sci.* **11**, 325 (2021).
18. Probst, H. et al. Unraveling femtosecond spin and charge dynamics with extreme ultraviolet transverse MOKE spectroscopy. Phys. Rev. Research **6**, 013107 (2024)
19. Carva, K., Legut, D. & Oppeneer, P. M. Influence of laser-excited electron distributions on the X-ray magnetic circular dichroism spectra: implications for femtosecond demagnetization in Ni. *EPL (Europhys. Lett.)* **86**, 57002 (2009).
20. Mathias, S. et al. Probing the timescale of the exchange interaction in a ferromagnetic alloy. *Proc. Natl. Acad. Sci. USA* **109**, 4792–4797 (2012).
21. Günther, S. et al. Testing spin-flip scattering as a possible mechanism of ultrafast demagnetization in ordered magnetic alloys. *Phys. Rev. B* **90**, 180407 (2014).
22. Radu, I. et al. Ultrafast and distinct spin dynamics in magnetic alloys. *SPIN* **05**, 1550004 (2015).
23. Hinzke, D. et al. Multiscale modeling of ultrafast element-specific magnetization dynamics of ferromagnetic alloys. *Phys. Rev. B* **92**, 054412 (2015).
24. Yao, K. et al. Distinct spectral response in M-edge magnetic circular dichroism. *Phys. Rev. B* **102**, 100405 (2020).
25. Jana, S. et al. A setup for element specific magnetization dynamics using the transverse magneto-optic Kerr effect in the energy range of 30-72 eV. *Rev. Sci. Instrum.* **88**, 033113 (2017).
26. Möller, C. et al. Ultrafast element-resolved magneto-optics using a fiber-laser-driven extreme ultraviolet light source. *Rev. Sci. Instrum.* **92**, 065107 (2021).
27. Jana, S. et al. Experimental confirmation of the delayed Ni demagnetization in FeNi alloy. *Appl. Phys. Lett.* **120**, 102404 (2022).
28. Dewhurst, J., Krieger, K., Sharma, S. & Gross, E. An efficient algorithm for time propagation as applied to linearized augmented plane wave method. *Comput. Phys. Commun.* **209**, 92–95 (2016).

29. Krieger, K., Dewhurst, J., Elliott, P., Sharma, S. & Gross, E. Laser-induced demagnetization at ultrashort time scales: predictions of TDDFT. *J. Chem. Theory Comput.* **11**, 4870–4874 (2015).
30. Bierbrauer, U. et al. Ultrafast magnetization dynamics in nickel: impact of pump photon energy. *J. Phys.: Condens. Matter* **29**, 244002 (2017).
31. Dewhurst, J. K. et al. Element specificity of transient extreme ultraviolet magnetic dichroism. *Phys. Rev. Lett.* **124**, 077203 (2020). 1909.00199.
32. Dewhurst, J. K. et al. The ELK code. elk.sourceforge.net (2018).
33. Koopmans, B. et al. Explaining the paradoxical diversity of ultrafast laser-induced demagnetization. *Nat. Mater.* **9**, 259–265 (2010).
34. Probst, H. et al. Replication data for: unraveling femtosecond spin and charge dynamics with EUV T-MOKE spectroscopy. https://doi.org/10.25625/CDBY3D GRO.Data (2023).
35. Minár, J., Mankovsky, S., Šipr, O., Benea, D. & Ebert, H. Correlation effects in fcc-Fe_xNi_{1-x} alloys investigated by means of the KKR-CPA. *J. Phys.: Condens. Matter* **26**, 274206 (2014).
36. Möller, C. et al. Replication data for: verification of ultrafast spin transfer effects in FeNi alloys. https://doi.org/10.25625/Z5TK24 GRO.Data (2024).

Acknowledgements

We thank Mario Fix and Manfred Albrecht from the University of Augsburg for the fabrication of the Fe–Ni samples. We also thank Thomas Brede from the Institut für Materialphysik Göttingen for the fabrication of the Ni sample. This work was funded by the Deutsche Forschungsgemeinschaft (DFG, German Research Foundation)—project IDs 399572199 and 432680300/SFB 1456. G.S.M.J. acknowledges financial support by the Alexander von Humboldt Foundation. S.S. and J.K.D. would like to thank the DFG for funding through project ID 328545488 TRR227 (project A04). We acknowledge support by the Open Access Publication Funds of the Göttingen University.

Author contributions

G.S.M.J., M.R., D.S., S.S. and S.M. conceived the research. C.M., H.P., M.S. and M.B. carried out the measurements. C.M., H.P. and G.S.M.J. performed the data analysis. J.K.D. and S.S. performed the TDDFT calculations. All authors discussed the results. G.S.M.J., D.S. and S.M. were responsible for the overall project direction. C.M., H.P., G.S.M.J. and S.M. wrote the manuscript with contributions from all co-authors.

Funding

Open Access funding enabled and organized by Projekt DEAL.

Competing interests

The authors declare no competing interests.

Additional information

Supplementary information The online version contains supplementary material available at https://doi.org/10.1038/s42005-024-01555-3.

Correspondence and requests for materials should be addressed to G. S. Matthijs Jansen or Stefan Mathias.

Peer review information *Communications Physics* thanks the anonymous reviewers for their contribution to the peer review of this work.